From the beam-envelope matrix to synchrotron-radiation integrals

Kazuhito Ohmi, Kohji Hirata, and Katsunobu Oide

KEK, National Laboratory for High Energy Physics, Oho, Tsukuba, Ibaraki 305, Japan
(Received 19 October 1992; revised manuscript received 19 May 1993)

The equilibrium state of an electron in a storage ring can be described most accurately by the envelope matrix, as long as the electron motion is linear. The equilibrium envelope can be calculated in the same way as the equilibrium barycenter (closed orbit). This is suited for accurate numerical calculations. The "emittances" can be extracted from the envelope as approximate quantities. The radiation integrals, which express the emittances in terms of Twiss parameters, dispersions, and other optical parameters, are extended to cover general 6×6 dynamics. Without any coupling between modes, these reduce to those of Sands.

I. INTRODUCTION

Future electron rings (flavor factories, damping rings of linear colliders, and synchrotron light sources) require quite accurate control of the equilibrium emittances and, more precisely, particle distribution to achieve high luminosity (for linear and circular colliders) or high brightness (for a synchrotron light source). The "emittance calculation" should become more accurate and more detailed. To be more precise, however, we should be more careful in using the concept of the emittance.

The most traditional approach is represented by the so-called radiation integrals [1], which express the emittances in terms of global optical quantities, such as three normal modes and their Twiss parameters, etc. Even if these traditional approaches give answers accurate enough in many cases, they are approximations and not the most direct way of determining the equilibrium beam distribution. They do not provide the "definition" of the equilibrium distribution.

The aim of this paper can be summarized as follows:

(1) We show how to calculate the equilibrium distribution of electron bunches as accurately as possible within a linear approximation. This is the envelope formalism. This is conceptually the most direct and practically, i.e., from a computational point of view, quite useful.

(2) We abstract the radiation integrals from the envelope formalism. As a result, we extend the synchrotron-radiation integrals as much as possible.

In Sec. II, we will discuss the envelope formalism. The synchrotron-radiation integrals will be discussed in Sec. III. The final section will be devoted to discussions and summary. Numerical examples of the envelope are given in the Appendix.

II. BEAM-ENVELOPE FORMALISM

The equilibrium distribution $\psi_\infty(\mathbf{x},s)$ should be defined by the solution of

$$\psi'(\mathbf{x},s)=\psi(\mathbf{x},s) , \qquad (1)$$

where ψ' is ψ after one revolution and $\mathbf{x}$ is the 6-tuple phase-space coordinate [2]. As long as we can assume that the major part of ψ is embedded in a region of phase space where the symplectic forces are linear, we can discuss $\psi_\infty(s)$ more directly: thanks to the central limit theorem, this $\psi_\infty(s)$ is Gaussian and can be represented by 21 second-order moments and 6 barycenter variables:

$$\psi(\mathbf{x};\bar{\mathbf{x}},\mathbf{R})=\frac{1}{(2\pi)^3\sqrt{\det R}}\exp[-\tfrac{1}{2}R_{ij}^{-1}(x-\bar{x})_i(x-\bar{x})_j] .$$

$$(2)$$

Here $\bar{\mathbf{x}}$ is the barycenter variable

$$\bar{\mathbf{x}}=\langle \mathbf{x} \rangle = \int \mathbf{x}\psi(\mathbf{x})d\mathbf{x} , \qquad (3)$$

and R is the envelope matrix

$$R_{ij}=\langle (x-\bar{x})_i(x-\bar{x})_j \rangle = \int (x-\bar{x})_i(x-\bar{x})_j\psi(\mathbf{x})d\mathbf{x} .$$

$$(4)$$

(Higher-order moments can be defined in the same way.) Since $R_{ij}=R_{ji}$, only 21 components are independent. Under this approximation, Eq. (1) is rewritten in a form

$$\bar{\mathbf{x}}'=\bar{\mathbf{x}}, \quad R'=R . \qquad (5)$$

Here we discuss how to determine the equilibrium barycenter and the equilibrium envelopes as accurately as possible within the linear approximation. We track the change of the beam barycenter $\bar{x}$ and envelope matrix R first through one element and later through one revolution to find the solution of Eq. (5). A computer code SAD [3] uses this method. See the Appendix. Ruggiero, Picasso, and Radicati [4,5] studied this approach independently.

A. Motion of an electron and coherent quantities

We first discuss the nonlinear dynamics of $\bar{x}$. We then evaluate the development of R in terms of quantities defined with respect to $\bar{x}$.

Imagine that we have a kind of optical element, a part of a magnet, a drift space, and so on. Each element is defined by two faces: an entrance face and an exit face.

A ring or a transport line is the summation of these elements.

Between the faces, the canonical variable $\mathbf{x}$ is defined. The single-particle dynamics treats an equation as

$$\frac{d\mathbf{x}(s)}{ds} = -[H(s),\mathbf{x}(s)] , \tag{6}$$

where H is the Hamiltonian representing the symplectic part of the motion and $[,]$ is the Poisson bracket:

$$[f,g] = \sum_{i,j} \partial_i f \partial_j g S_{ij} . \tag{7}$$

Here S is a matrix defined as

$$S = \mathrm{diag}(S_2, S_2, S_2), \quad S_2 = \begin{vmatrix} 0 & 1 \\ -1 & 0 \end{vmatrix} . \tag{8}$$

This induces a map from the entrance face to the exit face:

$$\mathbf{x}_{\mathrm{ent}} \rightarrow \mathbf{x}_{\mathrm{exit}} . \tag{9}$$

This map is symplectic:

$$\mathcal{M} S \mathcal{M}^t = S , \tag{10}$$

where $\mathcal{M}$ is the Jacobi matrix

$$\mathcal{M} = \frac{\partial(\mathbf{x}_{\mathrm{exit}})}{\partial(\mathbf{x}_{\mathrm{ent}})} . \tag{11}$$

The synchrotron-radiation perturbs this motion. As a result, the motion becomes stochastic. It is described by a stochastic equation

$$\frac{d\mathbf{x}}{ds} = -[H(\mathbf{x},s),\mathbf{x}] + \xi(\mathbf{x},s) , \tag{12}$$

where ξ is a stochastic variable describing the effects of the emission of photons. The latter depends on $\mathbf{x}$ and s. (Imagine, for example, the radiation in a quadrupole magnet.)

Because of its stochastic nature, we are forced to consider coherent or statistical quantities: the barycenter $\bar{\mathbf{x}}$, Eq. (3), the envelope R, Eq. (4), and in general higher-order coherent quantities. It is convenient here to define two averages: the average over the distribution ψ is $\langle\ \rangle^\psi$ and that over all possible ways of photon emission is $\langle\ \rangle^\gamma$. The double average is written simply as $\langle\ \rangle$.

We first discuss $\bar{\mathbf{x}}$, Eq. (3). Imagine that a distribution ψ_{ent} appears at the entrance face. This has the barycenter $\bar{\mathbf{x}}_{\mathrm{ent}}$. Let us discuss its value at the exit. From Eq. (12), we find

$$\frac{d\langle\mathbf{x}\rangle}{ds} = -\langle[H(\mathbf{x},s),\mathbf{x}]\rangle + \langle\xi(\mathbf{x},s)\rangle . \tag{13}$$

Since $\langle\partial H/\partial x_i\rangle = \partial\langle H\rangle/\partial\bar{x}_i$, we have

$$\langle[H(\mathbf{x},s),\mathbf{x}]\rangle = [\langle H(\mathbf{x},s)\rangle,\bar{\mathbf{x}}]' , \tag{14}$$

where

$$\langle H(\mathbf{x},s)\rangle = \int d\mathbf{x}\,\psi(\mathbf{x},s;\bar{\mathbf{x}},R,\dots)H(\mathbf{x},s) \tag{15}$$

is a function of $\bar{\mathbf{x}}$ and other statistical quantities and $[,]'$

is $[,]$ except that the differentiations are performed with respect to $\bar{\mathbf{x}}$. Thus, in general, the barycenter and a particle follow different paths even if they were identical at the entrance face. This difference becomes remarkable only when a nonlinearity is large and the force changes rapidly within the particle distribution. A typical example is the beam-beam kick [6], which we do not consider in this paper. Here, we assume this effect small so that

$$[\langle H(\mathbf{x},s)\rangle,\bar{\mathbf{x}}]' \simeq [H(\bar{\mathbf{x}},s),\bar{\mathbf{x}}]' . \tag{16}$$

That is, we assume that the barycenter motion is determined only by the barycenter and is independent from higher-order moments. Further discussion will be given in Sec. II D.

The second term in Eq. (13) has a similar property. That is, when the amount of radiation depends on the position too much, we should take this averaging seriously. The only example, at present, is the final focus quadrupole magnet near the limit of strong focusing [7]. We here ignore it also and assume that

$$\langle\xi(\mathbf{x},s)\rangle \simeq \xi_c(\bar{\mathbf{x}},s) \equiv \langle\xi(\bar{\mathbf{x}},s)\rangle^\gamma . \tag{17}$$

The equation of the barycenter now becomes

$$\frac{d\bar{\mathbf{x}}}{ds} = -[H(\bar{\mathbf{x}},s),\bar{\mathbf{x}}]' + \xi_c(\bar{\mathbf{x}},s) . \tag{18}$$

This is a deterministic equation and defines a trajectory of $\bar{\mathbf{x}}$ between the entrance and exit faces.

Let us turn to R. We linearize the motion of $\mathbf{x}$ around $\bar{\mathbf{x}}$. By using variables,

$$\mathbf{X} = \mathbf{x} - \bar{\mathbf{x}} , \tag{19}$$

the classical linearized motion of each particle obeys

$$\frac{d\mathbf{X}_c}{ds} = [S\hat{H}(s;\bar{\mathbf{x}}) - D(s;\bar{\mathbf{x}})]\mathbf{X}_c . \tag{20}$$

Here $\mathbf{X}_c = \langle\mathbf{X}\rangle^\gamma$, $\hat{H}(s;\bar{\mathbf{x}})$ is a symmetric 6×6 matrix,

$$\hat{H}(s;\bar{\mathbf{x}})_{ij} = \frac{1}{2}\left|\frac{\partial}{\partial x_i\partial x_j}H(\mathbf{x},s)\right|_{\mathbf{x}=\bar{\mathbf{x}}} , \tag{21}$$

and

$$D_{ij}(s;\bar{\mathbf{x}}) = -\left|\frac{\partial\xi_i^c(\mathbf{x},s)}{\partial x_j}\right|_{\mathbf{x}=\bar{\mathbf{x}}} . \tag{22}$$

The matrix D is called a damping matrix and causes the radiation damping. The off-diagonal terms of D produce a mixing between degrees of freedom, even if the symplectic part does not have any coupling terms. Its explicit form depends on the definition of $\mathbf{x}$ between both faces. In the matrices $\hat{H}$ and D, $\bar{\mathbf{x}}$ was written to note that they are evaluated on $\bar{\mathbf{x}}$. Hereafter, $\bar{\mathbf{x}}$ is always assumed and will be omitted in the arguments, unless it seems useful to stress $\bar{\mathbf{x}}$.

The solution of Eq. (2) can be written as

$$\mathbf{X}_c(s) = M(s,s')\mathbf{X}_c(s') , \tag{23}$$

where $M(s,s')$ is the transfer matrix with the damping effect,

$$M(s,s') = T \exp\left\{\int_{s'}^{s} [S\hat{H}(s'') - D(s'')] ds''\right\} . \quad (24)$$

Here T stands for the time-ordered product with respect to s. The transfer matrix M is not (but actually very close to) symplectic due to the presence of D.

The equation (12) is now replaced by

$$\frac{d\mathbf{X}}{ds} = [S\hat{H}(s) - D(s)]\mathbf{X} + \boldsymbol{\xi}(\mathbf{x},s) - \boldsymbol{\xi}_c(\bar{\mathbf{x}},s) . \quad (25)$$

We introduce another approximation that

$$\boldsymbol{\xi}(\mathbf{x},s) - \boldsymbol{\xi}_c(\bar{\mathbf{x}},s) \simeq \boldsymbol{\xi}(\bar{\mathbf{x}},s) - \boldsymbol{\xi}_c(\bar{\mathbf{x}},s) = \hat{\boldsymbol{\xi}}(\bar{\mathbf{x}},s) . \quad (26)$$

We evaluate the fluctuation term at $\bar{\mathbf{x}}$. Thus, this term does not depend on $\mathbf{X}$ so that Eq. (26) can readily be solved as

$$\mathbf{X}(s) = M(s,s_0;\bar{\mathbf{x}})\mathbf{X}(s_0) + \int_{s_0}^{s} M(s,s';\bar{\mathbf{x}})\hat{\boldsymbol{\xi}}(s;\bar{\mathbf{x}})ds' . \quad (27)$$

It can be shown that

$$\langle \hat{\boldsymbol{\xi}}(s_1;\bar{\mathbf{x}})\hat{\boldsymbol{\xi}}^t(s_2;\bar{\mathbf{x}})\rangle_c^\gamma = B(s_1;\bar{\mathbf{x}})\delta(s_1 - s_2) , \quad (28)$$

where B is a symmetric matrix called the diffusion matrix. Here $\langle AB \rangle_c$ stands for the average $\langle AB \rangle - \langle A \rangle\langle B \rangle$. Since $R_{ij} = \langle X_i X_j \rangle$, its time evolution is found from Eq. (27) as

$$R(s) = M(s,s_0)R(s_0)M^t(s,s_0) + \int_{s_0}^{s}\int_{s_0}^{s} M(s,s_1)\langle\boldsymbol{\xi}(s_1)\boldsymbol{\xi}(s_2)^t\rangle_c M^t(s,s_2)ds_1 ds_2$$

$$= M(s,s_0)R(s_0)M^t(s,s_0) + \int_{s_0}^{s} M(s,s')B(s')M^t(s,s')ds' . \quad (29)$$

We denote it in a concise manner [8]

$$R(s) = M(s,s_0)R(s_0)M^t(s,s_0) + \bar{B}(s,s_0) , \quad (30)$$

where a matrix $\bar{B}(s,s_0)$ is the integrated diffusion matrix:

$$\bar{B}(s,s_0) = \int_{s_0}^{s} M(s,s')B(s')M^t(s,s')ds' . \quad (31)$$

We thus have arrived at the expression of the mapping

$$(\bar{\mathbf{x}},R)_{\text{ent}} \to (\bar{\mathbf{x}},R)_{\text{exit}} . \quad (32)$$

$\bar{\mathbf{x}}_{\text{exit}}$ is a nonlinear function of $\bar{\mathbf{x}}_{\text{ent}}$ and it is obtained by the solution of Eq. (18): we denote it as

$$\bar{\mathbf{x}}_{\text{exit}} = \mathbf{f}(\bar{\mathbf{x}}_{\text{ent}}) . \quad (33)$$

On the other hand, R_{exit} is given by

$$R_{\text{exit}} = M(s_{\text{exit}}, s_{\text{ent}})R_{\text{ent}}M^t(s_{\text{exit}}, s_{\text{ent}}) + \bar{B}(s_{\text{exit}}, s_{\text{ent}}) . \quad (34)$$

The change of $(\bar{\mathbf{x}}, R)$ can be calculated only from the physical and local data of the element and $(\bar{\mathbf{x}}, R)_{\text{ent}}$.

We have employed several simplifications. They are all sorts of linearizations and are necessary to arrive at a linear system of envelope dynamics. More precisely, we kept the largest generality within a condition that if ψ is Gaussian at the entrance, it is still so at the exit. These should always be used with careful attention to their limits of validity. For example, the nonlinear wiggler [9] cannot be treated by the envelope formalism in the present form.

B. Explicit forms of damping and diffusion matrices

The previous discussion was general within the linear approximation. In order to give more explicit expressions, we should fix the variables.

From the entrance to the exit of the element considered here, we define a reference frame of coordinates. The choice is completely arbitrary [10]. Here, for illustration, we employ a straight line. (This can be used al-

ways: in bending magnets, quadrupole and higher-multipole magnets, solenoids, etc. In some cases, of course, this is not the most clever choice, but it is still usable.) We chose two orthonormal unit vectors $\mathbf{e}_x$ and $\mathbf{e}_y$. The so-called time variable s is the length along this line.

Once the spacial coordinates are defined, the motion of an electron is described by six variables $\mathbf{x}(s) = (x,p_x,y,p_y,z,\delta)$ as functions of s, the position in the ring. The momenta p_x and p_y are defined as x and y components of the relativistic 3-momentum normalized by the design momentum p_0:

$$p_{x,y} = \frac{[\mathbf{K} + e\,\mathbf{A}(x,y,s)]\cdot\mathbf{e}_{x,y}}{p_0} , \quad (35)$$

where e is the electron charge, $\mathbf{K}$ is the relativistic kinetic momentum ($m\gamma\,dx/dt$: m is the electron mass and γ the relativistic Lorentz factor), and $\mathbf{A}$ is the vector potential. The third pair z and δ are defined, respectively, as the difference in path length with respect to a reference particle and its canonical conjugate:

$$\delta = \frac{|\mathbf{K}| - p_0 - e\Phi(x,y,s)/c}{p_0}$$

$$= \frac{E - E_0 - e\Phi(x,y,s)}{E_0} , \quad E_0 = cp_0 , \quad (36)$$

where c is the light speed and Φ is the scalar potential. In this coordinate frame, we have the Hamiltonian

$$H(x,y,z,p_x,p_y,\delta) = \delta - eA_s/p_0$$

$$-\{(1+\delta+e\Phi/cp_0)^2$$

$$-(p_x - eA_x/p_0)^2$$

$$-(p_y - eA_y/p_0)^2\}^{1/2} , \quad (37)$$

where Φ is the scalar potential and $A_s = \mathbf{A}\cdot(\mathbf{e}_x \times \mathbf{e}_y)$. We have employed the ultrarelativistic limit ($\gamma \gg 1$) for the sake of simplicity. The reference particle is a nominal unphysical particle which runs on the reference line, with

a constant velocity. We will call these coordinates the physical variables in order to distinguish them from the betatron variables, for example.

A photon is emitted in the direction of the motion of the electron. Let $(|\mathbf{q}|,\mathbf{q})$ be the 4-momentum of the photon. We assume it to be real (not virtual). Since approximately $\mathbf{q}\|\mathbf{K}$, emission of a photon induces a change in $\mathbf{K}$ according to

$$\mathbf{K}\rightarrow\mathbf{K}-\mathbf{q}=\mathbf{K}-\frac{u(\mathbf{x},s)}{c}\frac{\mathbf{K}}{|\mathbf{K}|} \ ,$$

$$|\mathbf{K}|\rightarrow|\mathbf{K}|-\frac{u(\mathbf{x},s)}{c} \ , \tag{38}$$

where $u=c|\mathbf{q}|$ is the energy of the emitted photon [11]. This induces a change in (p_x,p_y,δ), other components being kept fixed. Here, we introduced a slight approximation that the electron is real (on-shell) both before and after the radiation. This breaks the energy-momentum conservation: we ascribe all the inconsistency to $K_s=\mathbf{K}\cdot(\mathbf{e}_x\times\mathbf{e}_y)$, because the latter is not what we track.

The stochastic variable $\xi(\mathbf{x},s)$ is now written as

$$\xi(\mathbf{x},s)=-\frac{u(\mathbf{x},s)}{E_0}\left[0,\frac{k_x}{1+\delta_k},0,\frac{k_y}{1+\delta_k},0,1\right]^t \ , \tag{39}$$

where $k_{x,y}=p_{x,y}-eA_{x,y}/p_0$ and $\delta_k=\delta+e\Phi/cp_0$ are regarded as functions of $\mathbf{x}$.

Here, u represents the stochasticity of ξ. The quantity u is stochastic in two different ways: whether a photon is emitted or not is stochastic and its energy is also stochastic when it is emitted. The former stochasticity is of Poisson distribution while the latter is governed by the radiation spectrum. We denote the average over the latter as $\langle\ \rangle^p$. To get the average $\langle\ \rangle^\gamma$, we need an averaging over time in addition. This problem is completely solved and the solution is known as the Campbell-Rice law [13]. Simple explanation can be found in Refs. [14,15] for the second-order moments. For more general cases used in accelerator contexts, see Refs. [13, 16–19]. The law tell us that

$$\langle\xi(\mathbf{x},s)\rangle^\gamma=N(\mathbf{x},s)\langle u(\mathbf{x},s)\rangle^p \ , \tag{40}$$

$$\langle u(\mathbf{x},s)u(\mathbf{x},s')\rangle^\gamma_c=N(\mathbf{x},s)\langle u^2(\mathbf{x},s)\rangle^p\delta(s-s') \ . \tag{41}$$

Here N is the photon number average for a unit length [20].

Thus, we have

$$\xi_c(\mathbf{x},s)=-\frac{N(\mathbf{x},s)\langle u(\mathbf{x},s)\rangle^p}{E_0}$$

$$\times\left[0,\frac{k_x}{1+\delta_k},0,\frac{k_y}{1+\delta_k},0,1\right]^t \ . \tag{42}$$

From the radiation spectrum, we have [20]

$$N(\mathbf{x},s)\langle u(\mathbf{x},s)\rangle^p=\frac{2}{3}\frac{r_e}{m}\gamma^2\left|\frac{p_0}{\rho_0(\mathbf{x},s)}\right|\frac{dl}{ds}$$

$$\equiv P(\mathbf{x},s) \ . \tag{43}$$

This quantity can be called the energy-loss rate. In the

above, $\rho_0(\mathbf{x},s)$ is the radius of the barycenter orbit, r_e is the classical electron radius, and l is the path length:

$$\frac{dl}{ds}=1-\frac{\partial H}{\partial\delta} \ . \tag{44}$$

Similarly, we have

$$N(\bar{\mathbf{x}},s)\langle u^2(\bar{\mathbf{x}},s)\rangle^p=\frac{55}{24\sqrt{3}}\frac{r_e\hbar}{m^2}\gamma^4$$

$$\times\left|\frac{p_0}{|\rho_0(\mathbf{x},s)|}\right|^3\frac{dl(\bar{\mathbf{x}},s)}{ds} \ . \tag{45}$$

From Eqs. (22), (42), and (43), we get

$$D_{ij}=\frac{1}{E_0}\frac{\partial}{\partial x_j}\left[P(\mathbf{x},s)\left[0,\frac{k_x}{1+\delta_k},0,\frac{k_y}{1+\delta_k},0,1\right]_i\right]_{\mathbf{x}=\bar{\mathbf{x}}} \ . \tag{46}$$

The explicit form of D_{ij} is generally quite lengthy. As is easily seen, we have $D_{1j}=D_{3j}=D_{5j}=0$. For example,

$$D_{21}=\frac{1}{E_0}P_{,x}\frac{\bar{k}_x}{1+\bar{\delta}_k}-\frac{P}{E_0}\left[\frac{a_{x,x}}{1+\bar{\delta}_k}+\frac{\bar{k}_x\phi_{,x}}{(1+\bar{\delta}_k)^2}\right] \ , \tag{47}$$

where $a_{x,x}=e/p_0\partial A_x/\partial x$, $P_{,x}=\partial P/\partial x$, and $\phi_{,x}=e/cp_0\partial\Phi/\partial x$. Also, $\bar{k}_x$ and $\bar{\delta}_k$ are k_x and δ_k of the barycenter.

The diffusion matrix is much simpler and is expressed as

$$B(s;\bar{\mathbf{x}})=\frac{N(\bar{\mathbf{x}},s)\langle u(\bar{\mathbf{x}},s)^2\rangle^p}{E_0^2}$$

$$\times\begin{vmatrix} 0 & 0 & 0 & 0 & 0 & 0 \\ 0 & \Delta^2\bar{k}_x^2 & 0 & \Delta^2\bar{k}_x\bar{k}_y & 0 & \Delta\bar{k}_x \\ 0 & 0 & 0 & 0 & 0 & 0 \\ 0 & \Delta^2\bar{k}_x\bar{k}_y & 0 & \Delta^2\bar{k}_y^2 & 0 & \Delta\bar{k}_y \\ 0 & 0 & 0 & 0 & 0 & 0 \\ 0 & \Delta\bar{k}_x & 0 & \Delta\bar{k}_y & 0 & 1 \end{vmatrix} \ , \tag{48}$$

where $\Delta=1/(1+\bar{\delta}_k)$.

We thus have given all necessary formulas to obtain explicit forms of D and B.

C. Barycenter and envelope in a transport line and a ring

1. Making a transport line

We have constructed a map of $(\bar{\mathbf{x}},R)$ for an element in a transport line, Eqs. (33) and (34). This map was constructed without knowing any data of the whole transport line. That is, the map is local.

Let us imagine that there are many elements in a series making a transport line or a ring. In order to construct a map for the whole line, we have only to apply the map successively. In doing it, however, care should be taken. To go from one element to the next, we should know the

relation between the two canonical variables in each element. The origin may be shifted or the definition of x and y may be rotated. The relation between two sets of (e_x, e_y) (displacement and rotation) is enough for us to construct the transformation between two canonical variables. (We do not have to know what kind of elements are connected.) This transformation is symplectic. (If the successive elements have employed different gauge, we should perform the gauge transformation at the same time.)

When the electron passes through two elements 1 and 2 successively, the total effects are

$$\bar{x}_{2(\text{exit})} = f_{1+2}(\bar{x}_{1(\text{ent})}) = f_2(T_{12} \circ f_1(\bar{x}_{1(\text{ent})})) , \tag{49}$$

$$R_{(\text{exit})} = M_2 T_{12}(M_1 R_{(\text{ent})} M_1^t + \bar{B}_1) T_{12}^t M_2^t + \bar{B}_2 , \tag{50}$$

where M_i and $\bar{B}_i$ are the M and $\bar{B}$ for the ith element. Here T_{12} is the transformation between $x_{1(\text{exit})}$ and $x_{2(\text{ent})}$ and T_{12} is its linearization.

Hereafter, for simplicity, we omit $\mathcal{T}$ and T, as we do in denoting a line on a manifold [21]. By repeating the similar transformations, we can obtain the map of $(\bar{x}, R)$ for the whole line.

2. One-turn map and equilibrium beam envelope

Let us consider the case where the exit of the transport line is identical to its entrance. That is a ring.

The evolution of $(\bar{x}, R)$ for one revolution of the ring is now expressed as

$$\bar{x}'(s) = \bar{x}(s + C) = f(\bar{x}(s)) , \tag{51}$$

$$R'(s) = R(s + C) = M(s) R(s) M^t(s) + \bar{B}(s) , \tag{52}$$

where C is the circumference (sum of the lengths of all the elements), $M(s) = M(s, s - C)$, and $\bar{B}(s) = \bar{B}(s, s - C)$.

By repeatedly applying Eq. (52), $(\bar{x}, R)$ at s will fall into an equilibrium [provided, of course, all the eigenvalues of $M(s)$ are less than unity in absolute value]. In the equilibrium, $(\bar{x}, R)$ takes the same value every turn so that this is a solution of

$$\bar{x}(s) = f(\bar{x}(s)) , \tag{53}$$

$$R(s) = M(s) R(s) M^t(s) + \bar{B}(s) . \tag{54}$$

The solution of Eq. (53) is the closed orbit of $\bar{x}$. By simplification of Eq. (16), we can solve it without knowing R. [Even without Eq. (16), we can still solve it together with R, if ψ can be assumed to be Gaussian.] Once $\bar{x}$ is fixed at s, we know it all around the ring. We use it to express M and $\bar{B}$ in Eq. (52). This is a linear equation and can be solved explicitly.

To express the solution in a concise manner, we introduce a 21-vector. For any symmetric 6×6 matrix A, we define

$$\vec{V}_A = (A_{11}, A_{11}, \ldots, A_{66})^t . \tag{55}$$

Correspondingly a 21×21 matrix $\tilde{M}$ is defined in such a way that

$$\tilde{M} \vec{V}_A = \vec{V}_{MAM^t} . \tag{56}$$

That is,

$$\tilde{M} = \begin{bmatrix} M_{11}^2 & M_{11}M_{12} & \cdots & M_{16}M_{16} \\ M_{11}M_{21} & M_{11}M_{22} & \cdots & M_{16}M_{26} \\ \vdots & \vdots & \ddots & \vdots \\ M_{61}M_{61} & M_{61}M_{62} & \cdots & M_{66}^2 \end{bmatrix} . \tag{57}$$

Thus Eq. (54) is cast in a simple form $\vec{V}_R = \tilde{M} \vec{V}_R + \vec{V}_{\bar{B}}$. The solution is simply

$$\vec{V}_R = \frac{I}{I - \tilde{M}} \vec{V}_{\bar{B}} . \tag{58}$$

With R, the beam size $\langle x^2 \rangle_c$ at s is obtained directly in terms of the physical variables without recourse to the emittances, betatron functions, and such. For example,

$$R_{11}(s) = \langle X^2 \rangle = \langle x^2 \rangle - \langle x \rangle^2 \tag{59}$$

is the horizontal beam size. The $R(s)$ at the other s can be obtained easily by using Eq. (30).

D. Comments on the equilibrium envelope

Several detailed discussions will be given.

1. Symplectic part of M

There may be several possible ways to define a symplectic transfer matrix from nonsymplectic matrix M. Here we give one definition for later convenience.

In each element, we make a large number of slices in the direction of s and assume that the radiation occurs only at the borders between the slices. Between the borders, a particle obeys the symplectic (nonlinear) equation. At each border, it is subject to the integrated (over the slice) effect of radiation. Let us denote the slices as an interval (s_{i-1}, s_i), where s_i's are points in the ring. The closed orbit of $\bar{x}$ includes all the nonlinear elements in the slices and the classical radiation effect at the borders.

In each slice (s_i, s_{i+1}) the dynamics remain symplectic. Let us linearize the dynamics around the closed orbit and denote the resulting matrix $M_0(s_{i+1}, s_i)$. Then the matrix M can be constructed as

$$M(s_n, s_0; \bar{x}) = \lim_{n \to \infty} \prod_{i=0}^{n-1} M_0(s_{i+1}, s_i; \bar{x})\{I - D(s_i; \bar{x}) ds_i\} , \tag{60}$$

where $ds_i = s_{i+1} - s_i$. We thus can define the symplectic revolution matrix $M_0(s)$ as

$$M_0(s; \bar{x}) = \lim_{n \to \infty} \prod_{\text{one turn}} M_0(s_{i+1}, s_i; \bar{x}) . \tag{61}$$

Here $\bar{x}$ was put in M_0 to stress that it is defined on the closed orbit. Note that the closed orbit depends on the radiation damping.

2. Emittances as approximate quantities

As we have seen in this section, the beam envelope at a particular location s, $R(s)$, is given as the solution of Eq. (54). This is a periodic function of s: the period is C.

Since the transfer matrix $M(s,s')$ is not symplectic and it does not commute with $B(s)$ (implying that it is impossible to diagonalize M and B simultaneously), there is not any constant of motion, like Courant-Snyder invariants for the symplectic dynamics. The emittances, thus, should be defined as approximate invariants, which are almost constant for the usual case when the damping is

much slower than the betatron and synchrotron oscillations.

We consider a (nonsymplectic and complex) transformation $V(s)$ which diagonalizes $M(s)$:

$$V(s)M(s)V^{-1}(s)=e^A ,\tag{62}$$

where A is a diagonal matrix:

$$A=\mathrm{diag}(i\mu_u-\alpha_u,-i\mu_u-\alpha_u,i\mu_v-\alpha_v,-i\mu_v-\alpha_v,i\mu_w-\alpha_w,-i\mu_w-\alpha_w) .\tag{63}$$

In this base, Eq. (54) can be solved more explicitly. Let us define

$$R_V(s)\equiv V(s)R(s)V^\dagger(s), \quad \bar{B}_V(s)\equiv V(s)\bar{B}(s)V^\dagger(s) .\tag{64}$$

Here $\dagger$ is the Hermite conjugate. Then Eq. (54) reads

$$R_V(s)=e^A R_V(s)e^{A^\dagger}+\bar{B}_V .\tag{65}$$

It is readily solved as

$$R_V^{ij}(s)=\frac{1}{1-e^{(A_{ii}+A_{jj}^*)}}\bar{B}_V^{ij}(s) .\tag{66}$$

Here $*$ is the complex conjugate. In particular, we have

$$R_V^{ii}(s)=\frac{1}{1-e^{-2\alpha_i}}\bar{B}_V^{ii}(s) .\tag{67}$$

The first term of Eq. (66) is of order unity in general. It can become large, however, if

$$|A_{ii}+A_{jj}^*|\ll 1 .\tag{68}$$

Now, let us introduce here a natural assumption that $\alpha_i\ll 1$, which is generally true for the usual accelerators. Let us ignore the case of the linear resonances [23]: i.e., the case with $\mu_i\simeq(\text{integer})\times 2\pi$ or $\mu_i\pm\mu_j\simeq(\text{integer})\times 2\pi$ for some i and j: The condition Eq. (68) is then satisfied if and only if $i=j$. We thus can conclude that

$$R_V=\mathrm{diag}(\epsilon_u,\epsilon_u,\epsilon_v,\epsilon_v,\epsilon_w,\epsilon_w)+O(\alpha\epsilon) ,\tag{69}$$

$$\epsilon_j=\frac{(V\bar{B}V^\dagger)_{jj}}{2\alpha_j} .\tag{70}$$

The emittances ϵ thus defined still depend on s weakly. Their variations as functions of s are of the order of α.

Note that the off-diagonal parts of $\bar{B}_V$ can easily become large, i.e., they can have magnitudes of the same order as the diagonal terms. They, however, do not contribute to the emittances except in the case of resonances. By the same reasoning, when the ring has a periodicity and the number of the period is large, $\bar{B}_V$ becomes almost diagonal [24].

The resonant case requires more careful treatment. As asserted in Ref. [4], it may be dangerous to represent the envelope by only three emittances.

In a coupling resonance $\mu_i\simeq\pm\mu_j$, if the tune difference $\mu_i\mp\mu_j$ can become comparable with or smaller than the damping rates, Eq. (68) does not hold true and $\bar{R}_V$ has off-diagonal terms comparable with diagonal terms. Examples are shown in the Appendix.

3. Eigenvalues

Since $M(s)$ is a real matrix, the eigenvalues are written in a form

$$\exp(\pm i\mu_k-\alpha_k), \quad k=u,v,w\tag{71}$$

as long as the motion is stable. Here $\alpha_k>0$ is the damping rate.

By performing the differentiations in Eq. (46), it can be proved that [15]

$$\mathrm{tr}D(s)=4\frac{P(\bar{x},s)}{E} ,\tag{72}$$

where P is the energy loss rate, Eq. (43), and $\bar{E}=E_0(1+\bar{\delta}_k)$. This equality holds true not only for the motion around the closed orbit but also for general cases (immediately after the injection, for example).

By using Eq. (60), it is easily shown that

$$\exp\left[2\sum_{k=u,v,w}\alpha_k\right]=\det\exp\left[\sum_i D(s_i)ds_i\right]$$

$$=\exp\left[\sum_i\mathrm{tr}D(s_i)ds_i\right] ,\tag{73}$$

so that we obtain [25]

$$\sum_{k=u,v,w}\alpha_k=2\frac{U_0}{\bar{E}} ,\tag{74}$$

where U_0 is the amount of radiation-energy loss per turn for the particle on the closed orbit. Needless to say, it is valid even when Φ, A_x, and A_y exist.

4. Nonlinearity in the barycenter motions

We have assumed Eq. (16). It is equivalent to assuming that the nonlinear force does not change its value considerably within the beam distribution. One important exception is the beam-beam force. Its effect on the closed orbit was discussed in Ref. [26]. Another possibly important example is a strong sextupole magnet. Even if the barycenter passes the center of the sextupole magnet, it receives a dipole kick. When the motion of a single particle is described as $x\to x+kx^2$, for example, we have

$$\bar{x}\to\bar{x}+k(\langle x^2\rangle_c+\bar{x}^2) .\tag{75}$$

Fortunately, this effect does not seem to be large in usual storage rings. For example, in design optics using the

TRISTAN main ring [27], the horizontal closed orbit distortion due to this kick is around 40 μm at the injection energy. It may be important, however, in the final focus system of future linear colliders. Inclusion of this effect in a computer code is easy. On the other hand, inclusion of a similar effect in the calculation of ψ seems quite difficult, because a non-Gaussian distribution emerges from a Gaussian one.

III. RADIATION INTEGRALS

In many cases, the damping is very slow and the radiation effect can be regarded as a small perturbation. Within this approximation, we can simplify the envelope calculation and the emittances, Eq. (70), can be expressed in terms of optical parameters. Here we express the emittances in terms of quantities of the symplectic dynamics, Twiss parameters, etc. This is essentially the radiation integrals. We will extend the radiation integrals considerably.

A. Symplectic normal modes

At a particular point s_0, it is always possible to find a complex matrix $V_0(s_0)$ for $M_0(s_0)$ which diagonalizes it:

$$V_0(s_0)M_0(s_0)V_0^{-1}(s_0)=U_0(s_0)\equiv e^{A_0} , \tag{76}$$

$$A_0=\text{diag}(i\mu_u^0,-i\mu_u^0,i\mu_v^0,-i\mu_v^0,i\mu_w^0,-i\mu_w^0) . \tag{77}$$

The diagonal terms of $\exp A_0$ are eigenvalues of $M_0(s_0)$.

The matrix $V_0(s_0)$ can be obtained by eigenvectors of $M_0(s_0)$ as

$$V_0^{-1}(s_0)=(\mathbf{v}_u,i\mathbf{v}_u^*,\mathbf{v}_v,i\mathbf{v}_v^*,\mathbf{v}_w,i\mathbf{v}_w^*) . \tag{78}$$

The eigenvectors are to be normalized as

$$\mathbf{v}_i^t S\mathbf{v}_j^* = -i\delta_{ij} \quad (i,j=u,v,w) . \tag{79}$$

This base defines the normal modes u, v, and w at s_0 and is called the normal mode base. There remains some ambiguity in defining $V_0(s_0)$: we can multiply the eigenvector $\mathbf{v}_i$ by any number of the form $\exp(i\phi_i)$. By Eq. (79), $V_0(s_0)$ satisfies the symplectic condition: $V_0^t SV_0=S$.

We recall Eq. (60) and employ the approximation that we ignore second- and higher-order terms in D in the product of it. We rewrite $M(s)$ as

$$M(s)=[I-\overline{D}(s)]M_0(s) , \tag{80}$$

$$\overline{D}(s)\simeq \int_{s-C}^{s}M_0(s,s_0)D(s_0)M_0^{-1}(s,s_0)ds_0\equiv \overline{D}_0(s) . \tag{81}$$

Let us define

$$\overline{\Lambda}(s_0)=V_0(s_0)\overline{D}_0(s_0)V_0^{-1}(s_0) . \tag{82}$$

Corresponding to Eq. (81), we have

$$U(s_0)\equiv V_0(s_0)M(s_0)V_0^{-1}(s_0)=[I-\overline{\Lambda}(s_0)]U_0(s_0) . \tag{83}$$

By the first-order perturbation, the eigenvalue of the matrix $U(s)$, which is equal to the eigenvalue of $M(s)$, is

given by

$$e^A=e^{A_0}[1-\overline{\Lambda}(s)_{ii}], \quad i=u,u^*,v,v^*,w,w^* . \tag{84}$$

Therefore the perturbed tune is given by

$$i\mu_i-\alpha_i=i\mu_{0i}-\overline{\Lambda}^{ii}(s) , \tag{85}$$

where $i\mu_{0i*}=-i\mu_{0i}$ and $\overline{\Lambda}_{i*i*}=\overline{\Lambda}_{ii}^*$. Thus we have

$$\alpha_i=\text{Re}[\overline{\Lambda}(s)_{ii}] \tag{86}$$

and

$$\mu_i=\mu_i^0-\text{Im}[\overline{\Lambda}(s)_{ii}] . \tag{87}$$

We also define

$$\overline{B}_0(s)=\int_{s-C}^{s}M_0(s,s')B(s')M_0^t(s,s')ds' \tag{88}$$

and

$$\overline{\Theta}(s)\equiv V_0(s)\overline{B}_0V_0^\dagger(s) . \tag{89}$$

As easily seen,

$$\overline{\Theta}(s)=V(s)\overline{B}(s)V^\dagger(s)[1+O(\alpha)] , \tag{90}$$

so that in the present approximation, we can identify these two.

Both the denominators and nominators of the emittances in Eq. (70) have been expressed by the normal mode bases. We thus have

$$\epsilon_i(s)\simeq \frac{\overline{\Theta}_{ii}(s)}{2\,\text{Re}[\overline{\Lambda}(s)_{ii}]}\equiv \overline{\epsilon}_i , \tag{91}$$

where $\epsilon_{i*}=\epsilon_i$ since $\overline{\Theta}_{i*i*}=\overline{\Theta}_{ii}$. We call it the perturbative emittance. In this approximation, the $\overline{\epsilon}$ is independent of s.

We   extend V_0 all   around   the   ring: $V_0(s)=M_0(s,s_0)V_0(s_0)$. Let us define

$$\Lambda(s)=V_0(s)D(s)V_0^{-1}(s) , \tag{92}$$

$$\Theta(s)=V_0(s)B(s)V_0^\dagger(s) . \tag{93}$$

As easily seen, we can rewrite Eqs. (82) and (88) as

$$\overline{\Lambda}_{ii}=\oint \Lambda(s)_{ii}ds , \tag{94}$$

$$\overline{\Theta}_{ii}=\oint \Theta(s)_{ii}ds . \tag{95}$$

Note that the definition of the phase advance is irrelevant for the calculations of these diagonal elements.

It can be seen that these are independent of s and so is the perturbed emittance, Eq. (91). Integrations using Eqs. (94) and (95) are employed in computer codes PETROC [28], SLIM [29] and also used in [30]. In order to calculate the equilibrium emittances, these are enough. (In some cases, however, the three emittances are not enough and we need the envelope formalism.) In the radiation integrals, our concern is not to calculate them but to express them by some optics parameters.

B. Diagonalization of the symplectic dynamics

We hope to express the numerator and denominator of Eq. (91) by Twiss parameters, phase advances, dispersion functions, and all such. These are widely used parameters of the linear symplectic dynamics. The definitions of these parameters, however, are not unique, especially in the case where dynamics is coupled in the six-dimensional phase space [31]. We thus should begin by defining them explicitly without any ambiguity. Here, we apply one possible way.

We have already constructed a symplectic complex matrix $V_0(s_0)$. Let us start by parametrizing it.

We prove that the matrix $V_0(s_0)$ can always be put in a form

$$V_0(s_0) = \tilde{P}(\phi_1,\phi_2,\phi_3)\tilde{B}(s_0)\tilde{R}(s_0)\tilde{H}(s_0) , \qquad (96)$$

where $\tilde{P},\tilde{B}$ (Twiss matrix), $\tilde{R}$ (Teng matrix), and $\tilde{H}$ (dispersion matrix) are 6×6 symplectic matrices ($\tilde{R}$ and $\tilde{H}$ being real):

$$\tilde{P}(\phi_1,\phi_2,\phi_3) = \exp[i(\phi_1,-\phi_1,\phi_2,-\phi_2,\phi_3,-\phi_3)] , \qquad (97)$$

$$\tilde{B} = \mathrm{diag}(B_u,B_v,B_w) , \qquad (98)$$

$$\tilde{R} = \begin{vmatrix} bI & S_2R_2^tS_2 & 0 \\ R_2 & bI & 0 \\ 0 & 0 & I \end{vmatrix} , \qquad (99)$$

$$\tilde{H} = \begin{vmatrix} \{1-|H_x|/(1+a)\}I & H_xS_2H_y^tS_2/(1+a) & -H_x \\ H_yS_2H_x^tS_2/(1+a) & \{1-|H_y|/(1+a)\}I & -H_y \\ -S_2H_x^tS_2 & -S_2H_y^tS_2 & aI \end{vmatrix} . \qquad (100)$$

Here B_i $(i=u,v,w)$, R_2, H_x, and H_y are 2×2 matrices:

$$B_i = \frac{1}{\sqrt{2}}\begin{vmatrix} \dfrac{1-i\alpha_i}{\sqrt{\beta_i}} & -i\sqrt{\beta_i} \\ \dfrac{-i+\alpha_i}{\sqrt{\beta_i}} & \sqrt{\beta_i} \end{vmatrix} , \qquad (101)$$

$$R_2 = \begin{vmatrix} r_1 & r_2 \\ r_3 & r_4 \end{vmatrix} , \quad H_k = \begin{vmatrix} \zeta_k & \eta_k \\ \zeta_k' & \eta_k' \end{vmatrix} . \qquad (102)$$

The suffix k means either x or y. Scalar parameters a in Eq. (100) and b in Eq. (99) are determined by the equations

$$a^2 + |H_x| + |H_y| = 1, \quad b^2 + |R_2| = 1 , \qquad (103)$$

respectively. Here α and β are real parameters and define the Twiss parameters [32] at s_0. The form of $\tilde{R}$ is due to Refs. [33] and [34].

To see that the decomposition Eq. (96) is possible, let us denote

$$\tilde{P}^{-1}V_0(s_0) = \begin{vmatrix} U_{11} & U_{12} & U_{13} \\ U_{21} & U_{22} & U_{23} \\ U_{31} & U_{32} & U_{33} \end{vmatrix} , \qquad (104)$$

where U_{ij} etc. are 2×2 submatrices. For the time being we assume that $|U_{33}|>0$, which implies that the x-z and y-z couplings are not very strong. (By the symplecticity of V_0, $|U_{ii}|$ is real) If we choose H_x and H_y as

$$H_x = -S_2U_{31}^tS_2U_{33}/a ,$$

$$H_y = -S_2U_{32}^tS_2U_{33}/a , \qquad (105)$$

$$a = \sqrt{|U_{33}|} ,$$

we can put

$$V_0(s_0)\tilde{H}^{-1}(s) = \begin{vmatrix} U_{11}' & U_{12}' & 0 \\ U_{21}' & U_{22}' & 0 \\ 0 & 0 & U_{33}/a \end{vmatrix} . \qquad (106)$$

The (3,1), (3,2), (1,3), and (2,3) elements in the above vanish due to the symplecticity of $V_0(s_0)$. We can further get

$$V_0(s_0)\tilde{H}^{-1}\tilde{R}^{-1} = \tilde{B}' = \mathrm{diag}(B_u',B_v',B_w') , \qquad (107)$$

by choosing

$$R_2 = -S_2U_{22}^tS_2U_{21}'/b, \quad b = \sqrt{|U_{22}'|} , \qquad (108)$$

where we have assumed that $|U_{22}'|>0$. Here the B''s are 2×2 symplectic matrices. Finally, if we choose three angles of $\tilde{P}$ properly, we arrive at the expression Eq. (101).

We have assumed

$$|U_{33}|>0, \quad |U_{22}'|>0 . \qquad (109)$$

Even if the conditions Eq. (109) break, we can do the decomposition after an appropriate redefinition or exchange of the eigenmodes at the location s. It is guaranteed by the fact that one of U_{31}, U_{32}, and U_{33} or one of U_{12}' and U_{22}' must have a positive determinant, because of the symplecticity of $V_0(s_0)$.

Now, we apply the same process to the matrix $M_0(s,s_0)V_0^{-1}(s_0)$: we put it in a form of Eq. (104) and find $V_0(s)$ and $\tilde{P}$ which satisfy

$$V_0^{-1}(s)\tilde{P}(\psi_u,\psi_v,\psi_w) = M_0(s,s_0)V_0^{-1}(s_0) . \qquad (110)$$

In this case, $\tilde{P}$ defines the phase advance of the modes.

Let us assume that $V_0(s)$ satisfies Eq. (109). [Let us call it (3-2) diagonalizable.] It may be true that $V_0(s)$ also satisfies $|U_{22}|>0$ and $|U_{11}'|>0$, i.e., it is (2-1) diagonalizable. That is, $V_0(s)$ is both (3-2) diagonalizable and (2-1) diagonalizable. All optical parameters in $\tilde{P}$, $\tilde{B}$, $\tilde{R}$, and $\tilde{H}$ in both schemes are related by a symplectic transformation. We can use either definition if we declare it explicitly. Thus, all optical parameters should have indices indicating the block elements used in the diagonalization: $\beta_u^{(3-2)}$, etc. If for $s_1 \leq s \leq s_2$, the (2-1) diagonalization was employed but (3-2) was used otherwise, the optical parameters jump from (3-2) to (2-1) at s_1 and return from (2-1) to (3-2) at s_2. That is, the optical parameters are discontinuous at s_1 and s_2. We will assume this convention and will omit the suffices like (3-2) below.

We thus expressed the transfer matrix as

$$M_0(s,s_0)=V_0(s)\tilde{P}(\psi_u(s,s_0),\psi_v(s,s_0),\psi_w(s,s_0))V_0^{-1}(s_0) \; ,$$

$$\tag{111}$$

where

$$V_0(s)=\tilde{B}(s)\tilde{R}(s)\tilde{H}(s) \; . \tag{112}$$

The definition Eq. (112) of the decomposition matrix looks reasonable, because it involves the conventional usage of dispersions η and η' and α and β functions at the weak-coupling limit.

$$H(x,y,z,p_x,p_y,\delta)=\delta-e\left[1+\frac{x}{\rho}\right]A_s/p_0-(xp_y-yp_x)/\tau$$

$$-\left[1+\frac{x}{\rho}\right]\{(1+\delta+e\Phi/cp_0)^2-(p_x-eA_x/p_0)^2-(p_y-eA_y/p_0)^2\}^{1/2} \; , \tag{113}$$

where ρ and τ are curvature radius and torsion of the closed orbit.

1. Diffusion matrix

Since $\tilde{k}$'s are zero on the closed orbit, only the (6,6) component remains in Eq. (48):

$$B(\bar{x}_0,s)=B_{66}1_{66} \; , \tag{114}$$

where 1_{66} is a matrix whose (6,6) element is 1 but other elements are zero, and

$$B_{66}=\frac{55}{24\sqrt{3}}\frac{r_e\hbar}{mc}\frac{\gamma^5}{|\rho|^3} \; . \tag{115}$$

Thus only the $(i,6)$ components of V_0 contribute to the matrix $\bar{\Theta}_{ii}$. In the present parametrization, these are written as

$$V_0^{16}(s)=-i[V_0^{26}(s)]^*=\frac{1}{\sqrt{2}}\left\{\frac{1-i\alpha_u}{\sqrt{\beta_u}}\eta_u-i\sqrt{\beta_u}\eta_u'\right\} \; ,$$

$$\tag{116}$$

$$V_0^{36}(s)=-i[V_0^{46}(s)]^*=\frac{1}{\sqrt{2}}\left\{\frac{1-i\alpha_v}{\sqrt{\beta_v}}\eta_v-i\sqrt{\beta_v}\eta_v'\right\} \; ,$$

$$\tag{117}$$

$$V_0^{56}(s)=-i[V_0^{66}(s)]^*=-\frac{i}{\sqrt{2}}a\sqrt{\beta_w} \; , \tag{118}$$

where η_u, η_u', η_v, and η_u' are "the dispersions of the eigenmodes" defined by

$$\begin{bmatrix}H_u\\H_v\end{bmatrix}\equiv\begin{bmatrix}bI & S_2R_s^tS_2\\R_2 & bI\end{bmatrix}\begin{bmatrix}H_x\\H_y\end{bmatrix} \; . \tag{119}$$

Note that $|H_u|+|H_v|=|H_x|+|H_y|=1-a^2$.

Using Eq. (117) we obtain the integral expression

C. Emittances

Let us express the integrals Eqs. (94) and (95) using optical parameters thus defined. This is a direct generalization of the method stated in [20]. Here we discuss the diagonal parts only, because off-diagonal parts are not necessary in expressing the emittances, although such an extension is easy.

Since D and B are defined on the closed orbit, it is useful to redefine the coordinates around it. We employ the Frenet-Serret construction of coordinates with respect to the closed orbit. Expressions in the preceding section are almost valid. The Hamiltonian now is

$$I_u\equiv\bar{\Theta}_{11}=\bar{\Theta}_{22}=\frac{1}{2}\oint\frac{\eta_u^2+(\beta_u\eta_u'+\alpha_u\eta_u)^2}{\beta_u}B_{66}ds \; ,$$

$$I_v\equiv\bar{\Theta}_{33}=\bar{\Theta}_{44}=\frac{1}{2}\oint\frac{\eta_v^2+(\beta_v\eta_v'+\alpha_v\eta_v)^2}{\beta_v}B_{66}ds \; , \tag{120}$$

$$I_w\equiv\bar{\Theta}_{55}=\bar{\Theta}_{66}=\frac{1}{2}\oint a^2\beta_wB_{66}ds \; .$$

2. Damping matrix

The damping matrix is still expressed by Eq. (46). Using that $k_x=0$ and $k_y=0$ on the closed orbit, we have

$$D(s)=\frac{P}{E_0}\begin{bmatrix}0 & 0 & 0 & 0 & 0 & 0\\-\Delta a_{x,x} & \Delta & -\Delta a_{x,y} & 0 & 0 & 0\\0 & 0 & 0 & 0 & 0 & 0\\-0\Delta a_{y,x} & 0 & -\Delta a_{y,y} & \Delta & 0 & 0\\0 & 0 & 0 & 0 & 0 & 0\\P^{-1}P_{,x} & 0 & P^{-1}P_{,y} & 0 & 0 & 2\Delta\end{bmatrix} \; , \tag{121}$$

where

$$P^{-1}P_{,x}=\frac{1}{P}\frac{\partial P}{\partial x}=\frac{1}{\rho}+\frac{2}{B_\perp}\frac{\partial B_\perp}{\partial x} \; , \tag{122}$$

$$P^{-1}P_{,y}=\frac{2}{B_\perp}\frac{\partial B_\perp}{\partial y} \; . \tag{123}$$

Here use is made of Eqs. (43) and (113) and we have used $\rho=p_0/eB_\perp$ ignoring the radiation in rf cavities.

Thus, the damping matrix D has only $D_{22}=D_{44}=D_{66}/2$, D_{21}, D_{23}, D_{41}, D_{43}, D_{61}, and D_{63} components. The contributions from both D_{21} and D_{43} to the $\text{Re}[\bar{\Lambda}_{ii}]$ are zero. The damping integrals are written as

$$\alpha_u = \text{Re}\overline{\Lambda}_{11} - \text{Re}\overline{\Lambda}_{22} = \tfrac{1}{4}\oint (1+|H_u|)D_{66}ds + \tfrac{1}{2}\oint \left[-b\eta_u + \frac{\eta_x |H_u|}{1+a} \right] D_{61}ds + \tfrac{1}{2}\oint \left[+b\eta_v - \frac{\eta_y(1+a-|H_u|)}{1+a} \right] D_{63}ds$$

$$- \tfrac{1}{2}\oint \left[br_2 a + \frac{f_{xy}(1+a-|H_u|)}{(1+a)^2} \right](D_{23}-D_{41})ds \ ,$$

$$\alpha_v = \text{Re}\overline{\Lambda}_{33} = \text{Re}\overline{\Lambda}_{44} = \tfrac{1}{4}\oint (1+|H_v|)D_{66}ds + \tfrac{1}{2}\oint \left[+b\eta_u - \frac{\eta_x(1+a-|H_v|)}{1+a} \right] D_{61}ds + \tfrac{1}{2}\oint \left[-b\eta_v + \frac{\eta_y |H_v|}{1+a} \right] D_{63}ds$$

$$- \tfrac{1}{2}\oint \left[-br_2 a + \frac{f_{xy}(1+a-|H_v|)}{(1+a)^2} \right](D_{23}-D_{41})ds \ , \tag{124}$$

$$\alpha_w = \text{Re}\overline{\Lambda}_{55} = \text{Re}\overline{\Lambda}_{66} = \tfrac{1}{4}\oint (1+a^2)D_{66}ds - \tfrac{1}{2}\oint a\eta_x D_{61}ds - \tfrac{1}{2}\oint a\eta_y D_{63}ds + \tfrac{1}{2}\oint f_{xy}(D_{23}-D_{41})ds \ ,$$

where

$$f_{xy} \equiv \zeta_x \eta_y - \eta_x \zeta_y \ . \tag{125}$$

The result satisfies Robinson's condition

$$\text{Re}[\overline{\Lambda}_{11} + \overline{\Lambda}_{33} + \overline{\Lambda}_{55}] = \oint D_{66}ds \ . \tag{126}$$

In summary, the perturbative emittances, Eq. (91), have been put in the form

$$\overline{\epsilon}_i = \frac{I_i}{2\alpha_i}(i = u,v,w) \ . \tag{127}$$

I_i is expressed by Eq. (120), while α_i is expressed by Eq. (124).

D. Reduction to simpler cases

In many cases, the coupling between transverse and longitudinal degrees of freedom are weak. If $\zeta = 0$ and $\zeta' = 0$, we have $|H_x| = 0$, $|H_y| = 0$, and $a = 1$. We thus have

$$\widetilde{H}(s) = \begin{vmatrix} I & 0 & -\boldsymbol{\eta}(s) \\ [S_2\boldsymbol{\eta}(s)]^t & 1 & 0 \\ \mathbf{0}^t & 0 & 1 \end{vmatrix} \ . \tag{128}$$

This happens when the dispersion function η vanishes in rf cavities. In this case, we have

$$\alpha_u = I_2 - I_u - I_s \ ,$$
$$\alpha_v = I_2 - I_v + I_s \ , \tag{129}$$
$$\alpha_w = 2I_2 + I_u + I_v \ ,$$

where

$$I_2 = \tfrac{1}{4}\oint D_{66}ds \ ,$$
$$I_u = \tfrac{1}{2}\oint [b\eta_u D_{61} + (\eta_y - b\eta_v)D_{63}]ds \ ,$$
$$I_v = \tfrac{1}{2}\oint [(\eta_x - b\eta_u)D_{61} + b\eta_v D_{63}]ds \ , \tag{130}$$
$$I_s = \tfrac{1}{2}\oint [br_2(D_{23}-D_{41})]ds \ .$$

The damping partition numbers are written as

$$(J_u, J_v, J_w) = \left[1 - \frac{I_u + I_s}{I_2}, 1 - \frac{I_v - I_s}{I_2}, 2 + \frac{I_u + I_v}{I_2} \right] \ . \tag{131}$$

If, further, we use the smooth approximation for the longitudinal motion, we get

$$\langle \delta^2 \rangle = \frac{\oint B_{66}ds}{4(2I_2 + I_u + I_v)} \tag{132}$$

and

$$\langle z_E^2 \rangle = \beta_w^2 \langle \delta^2 \rangle \ , \tag{133}$$

where

$$z_E = z + (x\eta_x' - p_x\eta_x + y\eta_y' - p_y\eta_y) \ . \tag{134}$$

Finally, without any coupling, the transfer matrix M_0 is written in a block diagonalized form. We have then further $R_2 = 0$, $b = 1$, $\eta_u = \eta_x$, and $\eta_v = \eta_y$. It is easy to see that all the radiation integrals reduce to those in Ref. [1].

IV. DISCUSSION

We have treated two different formalisms: the envelope formalism in Sec. II and the radiation integrals in Sec. III.

The radiation integrals were derived from the envelope formalism as approximate quantities. In deriving them, we have lost some information so that the opposite direction is impossible. Our radiation integrals are already extended considerably. Further extension may be done but it cannot become more accurate than the envelope formalism. The synchrotron-radiation integrals are of course useful. They are practically useful when, for example, we need rough lattice parameters which may provide some desired emittances for a perfect machine. In this case, the radiation integrals are useful only when they are simple. [We can express the off-diagonal terms of R_V, Eq. (66), in terms of optics parameters. This may generalize the radiation integrals and they are more accurate. It seems, however, that the expressions are too complicated and not quite useful in the design stage.] They may be also useful in perturbative approach, for ex-

ample, when we want to understand what kind of errors are dangerous for a blowup of the emittances. They are not useful, however, in calculating ψ_∞ accurately. It is dangerous to use them without noting that they are approximations and without paying attention to the border beyond which the approximations fail.

The envelope formalism is more general. It can be applied even when the damping is extremely fast. Any linear resonance does not cause trouble. In other words, if there were a divergence in the envelope calculation, this would be a real, physical phenomenon. The same formalism can also be used in calculating the intrabeam and/or Touschek effects, as SAD does. In this case, the Gaussian approximation should be imposed by hand.

There is another difference: the envelope formalism relies only on local quantities [22]. To study their motions, all we need is the local quantities, like the field strength. The definitions and translation law, Eq. (50), are valid whether the beam is in a ring or in a transport line. We can construct the one-turn map of R and $\bar{x}$ by simply performing the transformations in each element successively. On the other hand, the radiation integrals rely on the global quantities like normal modes defined by the symplectic part M_0 and defined around the closed orbit. To define it, we need information all over the ring.

Because of the local property of the envelope formalism, it is quite suited to numerical calculations: the calculation of making the one-turn map and that of finding equilibrium value are completely separated. This fact is well known for $\bar{x}$. We do not need the normal modes, etc. to find the closed orbit. The envelope is treated in exactly the same manner. If one has a tracking code for x, it should be quite easy to convert it to the tracking code for R. For any new type of ring element, as long as we know how to track a particle motion through it, we can also track the motion of R through it.

In order to illustrate the difference between two formalisms, let us imagine that we insert a thin quadrupole magnet in the center of the closed orbit at s, where the dispersion and coupling may exist. In order to calculate its effect on $R(s)$, all we need is the insertion strength K (a matrix), the revolution matrix before the insertion $M(s)$, and the integrated diffusion matrix $\bar{B}(s)$, which is not affected by the insertion. We can calculate the new envelope R_{new} by solving [35]

$$R_{new}(s)=M(s)KR_{new}(s)[M(s)K]^t+\bar{B}(s) ,\qquad (135)$$

instead of

$$R_{old}(s)=M(s)R_{old}(s)M^t(s)+\bar{B}(s) .\qquad (136)$$

On the other hand, in the radiation-integral formalism, we should first recalculate all the optical parameters throughout the ring, new principal modes, new β's, new η's, and so on. In addition, we should perform the integrals again. The latter is more complicated and is still less accurate. In this case, the use of the radiation integrals is an unnecessary detour.

A numerical example of the envelope and the conventional synchrotron-radiation integrals are shown in the Appendix for realistic ring parameters.

ACKNOWLEDGMENTS

APPENDIX; ENVELOPES IN SAD

The computer code SAD (Strategic Accelerator Design) [3] has been using the envelope formalism since 1987. (Afterwards, the synchrotron-radiation integrals were in-

TABLE I. The closed orbit, the symplectic part M_0 of M, and some optics parameters. The numbers in brackets denote multiplicative powers of 10.

	x	p_x/p_0	y	p_y/p_0	z	dp/p_0
			Closed orbit			
Entrance	$1.373[-5]$	$1.808[-7]$	$3.070[-8]$	$6.363[-9]$	$-1.193[-4]$	$4.723[-4]$
Exit	$1.373[-5]$	$1.808[-7]$	$3.070[-8]$	$6.363[-9]$	$-1.193[-4]$	$4.723[-4]$
			Symplectic part of the transfer matrix			
x	$-0.001\,303$	$5.617\,656$	$0.046\,268$	$0.910\,642$	$0.002\,666$	$0.025\,313$
p_x/p_0	$-0.182\,901$	$-0.010\,729$	$0.027\,934$	$-0.044\,668$	$5.085[-6]$	$0.005\,401$
y	$0.040\,748$	$0.914\,161$	$0.046\,834$	$5.894\,994$	$6.767[-6]$	$-0.001\,211$
p_y/p_0	$0.028\,355$	$-0.038\,875$	$-0.174\,197$	$0.013\,122$	$-3.264[-7]$	$-8.148[-4]$
z	$-0.005\,227$	$-0.027\,922$	$7.959[-4]$	$-0.001\,405$	$0.932\,765$	$-1.875\,072$
dp/p_0	$1.108[-5]$	$-0.002\,671$	$-4.605[-7]$	$-6.973[-6]$	$0.091\,258$	$0.888\,617$
			Parameters			

Design momentum	$P_0=10.0000$ GeV	Revolution frequency	$f_0=993\,25.2$ Hz
Energy loss per turn	$U_0=20.6482$ MV	Effective voltage	$V_c=90.0000$ MV
Stationary position	$dz=21.7188$ mm	Momentum compact.	$\alpha=6.43[-4]$
Orbit dilation	$dl=0.000\,00$ mm	Effective harmonic No.	$h=5120.00$
Bucket height	$dV/P_0=0.034\,03$		

TABLE II. The eigenvalues and eigenvectors of M_0. The latter is shown in the form of $\mathscr{E}^{-1}$. The numbers in brackets denote multiple powers of 10.

			Eigenvalues and eigenvectors			
Real	−0.005 803 1	−0.005 803 1	0.029 765 2	0.029 765 2	0.910 691 1	0.910 691 1
Imaginary	0.999 983 2	−0.999 983 2	0.999 556 9	−0.999 556 9	−0.413 088 1	0.413 088 1
Imaginary tune	0.000 000 0		0.000 000 0		0.000 000 0	
Real tune	0.250 923 6		0.245 262 0		−0.677 749	

	X	P_x	Y	P_y	Z	P_z
x	2.356 799	0.000 000	0.250 868	−0.020 402	7.225[−4]	0.013 628
p_x/p_0	−7.190[−4]	0.426 843	−0.013 885	−0.022 723	−4.586[−6]	4.450[−5]
y	0.129 128	−0.020 992	2.424 971	0.000 000	8.872[−7]	2.129[−5]
p_y/p_0	−0.013 772	−0.044 101	−0.006 602	0.414 844	4.607[−8]	−1.602[−6]
z	−2.445[−4]	0.012 392	−4.190[−4]	−6.390[−4]	2.130 618	0.000 000
dp/p_0	−7.699[−6]	1.135[−6]	−7.080[−7]	5.462[−8]	0.025 080	0.469 347

	x	p_x/p_0	y	p_y/p_0	z	dp/p_0
x	0.426 843	0.000 000	−0.044 101	0.020 992	1.135[−6]	−0.012 392
P_x	7.190[−4]	2.356 799	0.013 772	0.129 128	7.699[−6]	−2.445[−4]
Y	−0.022 723	0.020 402	0.414 844	0.000 000	5.462[−8]	6.390[−4]
P_y	0.013 885	0.250 868	0.006 602	2.424 971	7.080[−7]	−4.190[−4]
Z	4.450[−5]	−0.013 628	−1.602[−6]	−2.129[−5]	0.469 347	0.000 000
P_z	4.586[−6]	7.225[−4]	−4.607[−8]	8.872[−7]	−0.025 080	2.130 618

cluded for users accustomed to such integrals.) The concept of tracking R itself has been used frequently in the context of transport lines. Computer codes such as TRANSPORT [36] and DIMAD [37] calculate it at the exit of the line R_{out} when it is given at the entrance R_{in}: SAD calculates the solution of $R_{\text{in}} = R_{\text{out}}$. In using it for a

ring, however, we should calculate the closed orbit and evaluate M and B on it.

In this appendix, we show how SAD calculates the equilibrium envelope and show a related part of its outputs. We use the TRISTAN SOR lattice [38] as the example. The source of the x-y coupling is some skew quadru-

TABLE III. The damping part $M - M_0$ in physical and diagonalizing bases. The damping rates, the real tunes, and the partition numbers are also shown. The numbers in brackets denote multiplicative powers of 10.

	x	p_x/p_0	y	p_y/p_0	z	dp/p_0
		Radiation part of the transfer matrix				
x	2.357[−4]	−0.005 277	−3.675[−5]	−7.914[−4]	−3.002[−6]	−1.195[−4]
p_x/p_0	2.054[−4]	−1.748[−4]	−3.517[−5]	3.511[−5]	1.632[−8]	−6.082[−6]
y	8.637[−6]	−0.001 036	−8.434[−5]	−0.006 134	−2.502[−9]	−6.796[−7]
p_y/p_0	−2.853[−5]	5.590[−5]	1.783[−4]	−4.320[−6]	1.281[−9]	8.591[−7]
z	3.341[−6]	−3.210[−5]	−1.101[−6]	2.739[−7]	7.046[−5]	0.004 670
dp/p_0	3.297[−6]	3.261[−6]	−3.529[−7]	−1.110[−6]	−1.023[−4]	−0.003 823

	X	P_x	Y	P_y	Z	P_z
X	2.361[−4]	−9.383[−4]	3.611[−5]	2.013[−5]	−3.675[−8]	−4.172[−7]
P_x	0.001 125	−1.791[−4]	−2.159[−5]	−1.377[−6]	1.465[−7]	2.648[−7]
Y	3.621[−5]	−2.170[−5]	−6.292[−5]	−0.001 041	4.265[−9]	−4.053[−8]
P_y	2.149[−5]	−1.585[−6]	0.001 021	−2.202[−5]	2.038[−8]	4.843[−8]
Z	−2.890[−6]	−5.084[−6]	−2.427[−7]	1.417[−7]	1.254[−4]	0.001 029
P_z	1.676[−5]	6.327[−7]	−3.135[−8]	−1.152[−6]	−6.753[−4]	−0.003 878

Damping per one revolution

X: −1.031 840[−03] Y: −1.031 896[−03] Z: −2.060 653[−03]

Tune shift due to radiation

X: −3.586 321[−06] Y: 1.871 788[−06] Z: 1.382 670[−07]

Damping partition number

X: 1.0007 Y: 1.0008 Z: 1.9985

TABLE IV. The integrated diffusion matrix in physical $(\bar{B})$ and diagonalizing bases $(\bar{B}_E)$. Symmetric matrices are shown in this way. The numbers in brackets denote multiplicative powers of 10.

| | Beam matrix by radiation fluctuation | | | | | |
	x	p_x/p_0	y	p_y/p_0	z	d_p/p_0
x	3.138[−11]					
p_x/p_0	1.336[−13]	5.602[−13]				
y	2.166[−12]	2.148[−13]	4.336[−13]			
p_y/p_0	−2.194[−14]	−3.754[−14]	−1.565[−14]	4.920[−15]		
z	−5.925[−10]	−2.571[−12]	−1.622[−12]	1.365[−13]	2.969[−08]	
dp/p_0	4.814[−10]	1.434[−12]	1.179[−12]	−9.117[−14]	−2.024[−08]	1.645[−08]

	X	P_x	Y	P_y	Z	P_z
X	3.072[−12]					
P_x	8.455[−14]	3.103[−12]				
Y	2.044[−13]	2.333[−13]	4.712[−14]			
P_y	9.628[−14]	1.241[−13]	1.590[−14]	2.181[−14]		
Z	−9.577[−13]	−6.346[−13]	−9.138[−14]	−2.517[−14]	6.541[−09]	
P_z	3.363[−12]	−9.203[−13]	1.990[−13]	−1.605[−13]	−2.058[−08]	7.685[−08]

pole magnets artificially inserted in the ring. The random alignment errors are not used in this example.

For each element, we introduce a longitudinal slicing, as in Sec. II D 1. The radiation is thought to occur at the borders between the slices and the dynamics is thought to be symplectic within the slice. Thus the orbit appears discontinuous (in phase space) at each border due to the radiation. For each slice, we prepare a map of $(\bar{x}, R)$ in terms of local coordinates. This includes the (in general nonlinear) map of $\bar{x}$ and M_0 for arbitrary orbit. The latter determines the transformation of R. At each border, we give mutual relations of x's between neighboring slices. (The alignment and tilt errors are included here). The classical radiation, Eq. (42), the matrix D, Eq. (46), and B, Eq. (48), are prepared at the border for an arbitrary value of $\bar{x}$. We track $\bar{x}$ for one turn from s_0 to

$s_0 + C$ to find its closed orbit, Eq. (53). Here s_0 is an arbitrary point and will be called the reference point (RP). As long as we employ the approximation of Eq. (16), this is equivalent to finding the closed orbit for a single particle with a damping effect. Then we track once again for one turn using the data of $\bar{x}$ to find $M(s_0; \bar{x})$ and $\bar{B}(s_0; \bar{x})$. Then we get the equilibrium value $R(s_0)$ by Eq. (54).

In Table I, the first part of SAD outputs is shown. The coordinates of the closed orbit at the RP are written. Here, the source of the closed orbit is only the radiation damping. Once the closed orbit is found, it calculates the symplectic revolution matrix $M_0(s_0)$ defined on it, Eq. (61). To evaluate the numerical errors, SAD shows $-JM_0JM_0^t$, which indicates how M_0 is symplectic. This part is omitted here. Some important parameters are shown also.

TABLE V. The equilibrium envelope R in diagonalizing and physical bases. The numbers in brackets denote multiplicative powers of 10.

| | Equilibrium beam matrix | | | | | |
	X	P_x	Y	P_y	Z	P_z
X	1.497[−09]					
P_x	−5.363[−13]	1.497[−09]				
Y	1.511[−12]	−3.547[−12]	1.673[−11]			
P_y	3.686[−12]	1.469[−12]	1.608[−14]	1.672[−11]		
Z	−1.315[−13]	4.058[−14]	−3.199[−16]	3.601[−16]	1.014[−05]	
P_z	7.326[−13]	1.484[−12]	1.040[−13]	2.836[−13]	−4.363[−11]	1.014[−05]

	x	p_x/p_0	y	p_y/p_0	z	dp/p_0
x	1.020[−08]					
p_x/p_0	2.357[−12]	2.727[−10]				
y	4.774[−10]	−1.782[−11]	1.253[−10]			
p_y/p_0	−4.530[−11]	−2.804[−11]	−1.014[−12]	5.974[−12]		
z	1.561[−08]	−9.112[−11]	1.856[−11]	1.861[−13]	4.603[−05]	
dp/p_0	6.503[−08]	2.109[−10]	1.016[−10]	−7.592[−12]	5.418[−07]	2.240[−06]

Emittance X	= 1.496 67[−9] m	Emittance Y	= 1.6728[−11] m
Emittance Z	= 1.013 82[−5] m	Energy spread	= 0.001 496 50
Bunch length	= 6.784 275 74 mm	Beam tilt	= −0.047 220 90 rad
Beam size ξ	= 0.101 129 54 mm	Beam size η	= 0.010 137 98 mm

In Table II, the eigenvalues and eigenvectors of M_0 are shown. The latter forms the transformation matrix to the real normal base $X_{\mathcal{E}} = \mathcal{E}X$, where $\mathcal{E}$ is defined in such a way that

$$\mathcal{E}M_0\mathcal{E}^{-1} = \text{diag}\left[\begin{bmatrix} \cos\mu_I & \sin\mu_I \\ -\sin\mu_I & \cos\mu_I \end{bmatrix}, \cdots \right]. \quad (A1)$$

The $\mathcal{E}$ is just the real representation of V_0, Eq. (78), and is related to V_0 by a complex symplectic similarity transformation. SAD shows $\mathcal{E}^{-1}$ which is composed of the eigenvectors.

The revolution matrix $M(s_0)$ is shown in the form of $M - M_0 = \bar{D}_0 M_0$, both in physical and diagonalizing bases. They are shown in Table III. As is clear from this example, the damping does not occur in the directions of the principal modes: it mixes the modes. Also the eigenvalues of M give the damping rates α's, Eq. (86), the real tune, Eq. (87), and the damping partition numbers.

The integrated diffusion matrix $\bar{B}(s_0)$, Eq. (31), and its normal base representation $\bar{B}_E = \mathcal{E}\bar{B}\mathcal{E}^t$ are shown in Table IV. From the latter, it should be noted that $\bar{B}_E$ can have rather large off-diagonal elements. It also mixes the modes.

Then the equilibrium envelope R is determined based on Eq. (58). It is shown both in the normal base $(R_E = \mathcal{E}R\mathcal{E}^t)$ and the physical base. See Table V. The diagonal terms of the normal bases give the emittances ϵ.

The equilibrium envelope in the normal base, R_E, is almost diagonalized but not completely so. For example, the (3,1) component is smaller than (1,1) but is not much smaller than (3,3). In fact,

$$|R_V^{31}| = \sqrt{R_E^{31}R_E^{42} - R_E^{32}R_E^{43}}$$

is almost as large as one-fourth of ϵ_V. In this optics, we cannot say that the envelope is well approximated by three emittances with enough accuracy. This tendency is enhanced near resonance [4].

The envelope formalism is not influenced by the resonance at all, provided all the eigenvalues of M are less than unity in absolute value. The equilibrium envelope, obtained by Eqs. (54) or (58), is always applicable. If the tune difference between two normal modes is smaller than the damping rate α, the off-diagonal elements of the envelope in the normal mode R_V are not reduced to be $O(\alpha)$. For example, if $|\mu_u - \mu_v| \lesssim \alpha$, the (1,3) and (2,4) components of R_V will remain large.

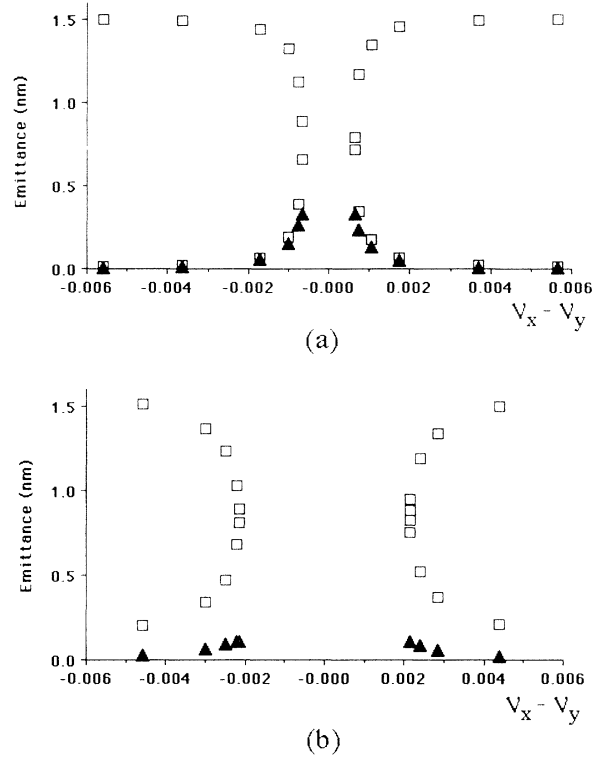In the above model, we surveyed emittances in a region

FIG. 1. Behaviors of emittances near difference resonances calculated by the envelope formalism (by SAD). (a) Horizontal-vertical coupling $(\nu_x \sim \nu_y)$. (b) Same as (a) but with skew quadrupole magnets three times stronger.

of $|\mu_x - \mu_y| \sim 0$. The desired tunes were achieved by the linear matching but with keeping the strength of the inserted skew quadrupole magnets constant. The emittances ϵ_u and ϵ_v (the diagonal parts of R_V) and $|R_V^{31}|$ are plotted as functions of $|\nu_u - \nu_v|$ in Fig. 1(a). The physical tunes cannot become identical so that there are no data for $\nu_u = \nu_v$. The minimum tune difference is of the order of the damping rate α. The $|R_V^{31}|$ becomes of the same order as the emittances. The envelope matrix for this case is shown in Table VI.

If the coupling source (the strength of the inserted skew quadrupoles) becomes stronger, the above effect becomes less remarkable. In fact, it seems that the minimum tune difference is larger for larger coupling strength. In Eq. (66), the $\bar{B}_V^{ij}$ is not much affected by the insertions. The denominator for R_V^{31},

$$1 - \exp[i(\mu_u - \mu_v) - (\alpha_u + \alpha_v)],$$

TABLE VI. The equilibrium envelope in the diagonalizing base , R_E, corresponding to the case where the tune difference is the minimum. The numbers in brackets denote multiplicative powers of 10.

			Equilibrium beam matrix			
	X	P_x	Y	P_y	Z	P_z
X	7.914[−10]					
P_x	−1.661[−13]	7.914[−10]				
Y	2.621[−10]	−2.043[−10]	7.223[−10]			
P_y	2.041[−10]	2.621[−10]	−1.067[−14]	7.222[−10]		
Z	−1.008[−13]	2.808[−14]	−6.710[−14]	5.899[−14]	1.014[−05]	
P_z	5.507[−13]	9.598[−13]	9.023[−13]	9.011[−13]	−2.186[−11]	1.014[−05]

determines it. Therefore, for larger values of the coupling strength, the maximum value of the $|R_V^{31}|$ as a function of the tune difference becomes smaller. Figure 1(b) is the same as Fig. 1(a) but with three times stronger inserted skew quadrupole magnets. The $|R_V^{31}|$ is smaller than

that for Fig. 1(a).

The assumption that the envelope is dominated by three emittances, implicitly used by the users of the radiation integrals, fails particularly when the coupling is weak and the physical tune difference becomes small.

[1] R. H. Helm, M. J. Lee, P. L. Morton, and M. Sands, IEEE Trans. Nucl. Sci. NS-20, 900 (1973).

[2] It is not evident whether Eq. (1) has a solution in general. The so-called dynamic aperture will bring a fraction of the particles far away from the origin and such particles never return. Also a chaotic region may make ψ a fractal function. We do not expect to have ψ_∞ as a usual function. Such cases are beyond the scope of this paper.

[3] A computer code SAD, Strategic Accelerator Design, has been built and used in KEK. For example, see K. Hirata, Proceedings of the 2nd International Committee for Future Accelerators Beam Dynamics Workshop, Lugano, 1988, edited by E. Keil and J. Hagel, CERN Report No. 88-04 (CERN, Geneva, 1988).

[4] F. Ruggiero, E. Picasso, and L. Radicati, Ann. Phys. (N.Y.) 197, 396 (1990).

[5] We have developed the envelope formalism and have installed it into SAD before Ref. [4]. We, however, did not publish it except for a brief discussion in Ref. [3]. The stress of the present paper is on the practical usefulness of the envelope formalism, while the authors of Ref. [4] are more interested in general formalism.

[6] K. Hirata, Nucl. Instrum. Methods Phys. Res. A 269, 7 (1988).

[7] K. Oide, Phys. Rev. Lett. 61, 1713 (1988); K. Hirata, B. Zotter, and K. Oide, Phys. Lett. B224, 437 (1989).

[8] F. Ruggiero and B. Zotter, CERN Report No. CERN/LEP-TH/88-33, 1988 (unpublished).

[9] For example, A. Hofmann and J. M. Jowett, CERN Report No. CERN/ISR-TH/81-23, 1981 (unpublished).

[10] In the general approach, we employ a line (straight or curved) from the entrance face to the exit face. For simplicity we use a line crossing both faces with a right angle. There is no need for this line to be a trajectory which obeys the equation of motion of a certain particle. The length of this line defines the so-called time variable s. There can be many ways to define coordinates around this line. One example: we define two transverse unit vectors e_x and e_y perpendicular to each other and parallel to the entrance face. We bring it to the exit face by the parallel transport along the reference line [12]. By this, the coordinates x and y are defined. Another example: we can define coordinates by Frenet-Serret construction based on the reference line. These coordinates can be chosen with respect to the easiness of integration of equations of motion.

[11] There are components of q transverse to K. This effect (opening angle) has been discussed in Ref. [20] and in T. Raubenheimer, Part. Accel. 36, 75 (1991). Since this effect is tiny in most cases, we ignore it. The envelope formalism, however, can treat this effect in a straightforward manner [K. Hirata, SLAC-Report No. AAS-Note 80, 1993 (unpublished)].

[12] K. Yokoya, KEK Internal Report No. 85-7, 1985 (unpublished).

[13] S. O. Rice, Bell Syst. Tech. J. 23, 282 (1944).

[14] M. Sands, Stanford Linear Accelerator Center Report No. SLAC/AP-47, 1985 (unpublished).

[15] J. M. Jowett, in Proceedings, Joint US-CERN School on Particle Accelerators, Santa Margherita di Pula, Sardinia, 1985, edited by J. M. Jowett, M. Month, and S. Turner, Lecture Notes in Physics Vol. 247 (Springer-Verlag, Berlin, 1986), p. 343.

[16] K. Hirata, CERN Report No. CERN/LEP-TH/89-03, 1989 (unpublished).

[17] K. Hirata and K. Yokoya, Part. Accel. 39, 147 (1992).

[18] T. O. Raubenheimer, KEK Report No. 92-7, 1992 (unpublished).

[19] Yu. P. Virchenko and Yu. N. Grigor'ev, Ann. Phys. (N.Y.) 209, 1 (1991).

[20] M. Sands, Stanford Linear Accelerator Center Report No. SLAC-121, 1970 (unpublished).

[21] This is a common notation in differential geometry. See the discussion on the fiber bundle description in Ref. [22].

[22] E. Forest and K. Hirata, KEK Report No. 92-12, 1992 (unpublished).

[23] G. Guignard, CERN Report No. CERN-76-06, 1976 (unpublished); LEP Note No. 154, 1979 (unpublished).

[24] K. Hirata and F. Ruggiero, Part. Accel. 28, 137 (1990).

[25] K. W. Robinson, Phys. Rev. 111, 373 (1958).

[26] K. Hirata, Part. Accel. 41, 93 (1993).

[27] Accelerator Design of the KEK B Factory, edited by S. Kurokawa, K. Satoh, and E. Kikutani, KEK Report No. 90-24 (KEK, Ibaraki, 1991).

[28] G. Guignard and Y. Marti, CERN Report No. CERN/ISR-BOM-TH/81-32, 1981 (unpublished).

[29] A. Chao, J. Appl. Phys. 50, 595 (1979). The approach in this paper can be understood as an intermediate between those in our Secs. II and III. Roughly speaking, it is closer to the envelope approach in that one tracks three emittances and finds their equilibrium values afterwards. On the other hand, it is closer to the radiation-integral approach in that only three emittances are concerned: one needs to know the principal modes in advance.

[30] D. P. Barber, K. Heinemann, H. Mais, and G. Ripken, DESY Report No. DESY91-146, 1991 (unpublished).

[31] For example, G. Ripken, DESY Report No. DESY R1-70/4, 1970 (in German, unpublished).

[32] E. D. Courant and H. S. Snyder, Ann. Phys. (N.Y.) 3, 1 (1958).

[33] L. Teng, Report No. FN-229, 1971 (unpublished); D. Edwards and L. Teng, IEEE Trans. Nucl. Sci. NS-20, 885 (1973).

[34] K. Yokoya (private communication).

[35] K. Hirata and F. Ruggiero, CERN Report, LEP Note No. 611, 1988 (unpublished).

[36] K. L. Brown, F. Rothacker, D. C. Carey, and Ch. Iselin, SLAC Report No. SLAC-91, Rev. 2, UC-28 (I/A) (1977) (unpublished).

[37] R. V. Servranckx, K. L. Brown, L. Schachinger, and D. Douglas, SLAC Report No. 285 UC-28 (A) (1985) (unpublished).

[38] S. Kamada and K. Ohmi, in Proceedings of Workshop on 4th Generation Light Sources, February, 1992, edited by M. Cornacchia and H. Winick, SSRL Report No. SSRL-92/02 106 (1992) (unpublished).